Design and Experimental Implementation of a Fuzzy Logic Controller for Shape Memory Alloy-Driven Robotic Arm

Motahareh Nasiri[a], Sadra Rafatnia[a*], Mehdi Mirzaei[a], Zahra Ahangari Sisi[a]

[a] *Faculty of Mechanical Engineering, Sahand University of Technology, 513351996, Tabriz, Iran.*

* *Corresponding author e-mail: sa_rafatnia@sut.ac.ir.*

Abstract

A robotic manipulator actuated by shape memory alloy (SMA) offers a lightweight and compact design but poses significant control challenges due to the material's inherent nonlinearities, such as hysteresis and slow cooling dynamics. This study deals with the design and experimental implementation of a fuzzy logic controller for the precise position control of an SMA-driven arm. The angular displacement of the robotic arm is measured using an encoder, which provides the feedback for the control system. The proposed fuzzy controller is designed with two input variables including the tracking error and its derivative and a single output for the command voltage. A rule base of 25 linguistic rules is constructed based on proportional-derivative (PD) control principles to effectively manage the SMA's nonlinear behaviour. Finally, the controller is implemented on a laboratory-scale manipulator, and experimental tests under step and sinusoidal reference trajectories are conducted. The results illustrate the good performance of the proposed control scheme, demonstrating superior tracking accuracy and reliability compared to a conventional PD controller.

Keywords: Fuzzy control; Shape memory alloy; Robotic arm; Experimental validation.

1. Introduction

Shape memory alloys (SMAs) are recognized as smart materials of critical importance in both scientific and industrial domains, primarily due to their extraordinary deformation capability upon thermal activation. Unlike traditional hydraulic or pneumatic actuators, SMAs offer a compelling combination of beneficial characteristics, including a high power-to-weight ratio, low energy consumption, minimal acoustic noise, and swift actuation. These properties make them exceptionally well-suited for demanding applications in advanced sectors such as robotics, aerospace, and automotive engineering [1].

However, the practical deployment of SMA actuators is complicated by a significant challenge due to their inherent hysteresis. This behaviour arises from a temperature-dependent, reversible phase transformation between martensite and austenite crystal structures, where the forward and reverse transformation paths do not coincide [2]. The resulting highly nonlinear and history-dependent response makes accurate modelling and precise control of SMA actuators a complex task.

In response to this challenge, a variety of nonlinear control strategies have been developed. The literature documents approach such as super-twisting sliding mode control [3], adaptive predictive control [4], non-singular terminal sliding mode control [5], and robust feedback control [6]. Liu et al. [7], for instance, contributed a prescribed performance adaptive sliding mode control scheme. A common thread among these advanced methods is their significant computational complexity, which is the price for achieving precise tracking and robustness against nonlinearities and hysteresis. Furthermore, many are explicitly model-based, leading to control laws that guarantee stability at the cost of potentially conservative performance, as they must account for system uncertainties and perturbations.

This study addresses these limitations by presenting the design and experimental validation of a Mamdani-type fuzzy logic controller (FLC) for the precise angular positioning of a robotic arm actuated by an SMA spring. The proposed FLC offers a model-free alternative, circumventing the need for a complex mathematical model and its associated uncertainties. In the developed prototype, an encoder provides real-time measurement of the arm's angular position. This feedback is processed by the FLC, which intelligently computes the appropriate actuation voltage for the SMA spring, effectively regulating its displacement. To rigorously evaluate performance, the proposed FLC is compared against a conventional proportional-derivative (PD) controller across diverse angular displacement profiles. The results demonstrate the FLC's superior effectiveness in managing the nonlinear hysteresis and transient response of the SMA actuator, providing more accurate and robust tracking performance. Therefore, the main contributions of this paper are presented as follows:

- The design and experimental implementation of a Mamdani-type fuzzy logic controller (FLC) for precise angular control of an SMA-actuated robotic arm.
- A comparative analysis demonstrating the FLC's superior performance in tracking complex trajectories and managing hysteresis compared to a conventional PD controller.

The organization of the paper is given as follows: Section 2 presents the overall structure of the used control system. Section 3 a brief overview of the mathematical model of the wire is discussed. Section 4 explains the design of the proposed controller. The experimental results of the proposed control method are presented in Section 5. Finally, the conclusion is given in Section 6.

2. Overall structure of the used control system

Figure 1 illustrates the comprehensive control system architecture employed in this study for the precise trajectory tracking of the SMA actuator-based robotic arm. The process begins at the experimental setup, where a high-resolution shaft encoder (600 pulses per revolution) continuously measures the angular position of the actuator at frequency of 50 Hz. This real-time positional data is acquired by an Arduino UNO microcontroller, which serves as the primary hardware interface. The Arduino then transmits the sensor readings to a computational upper layer via a serial communication link. Within the MATLAB/Simulink environment, this feedback signal is compared against a predefined reference trajectory to generate a position error. This error is fed into a sophisticated fuzzy logic controller block, which intelligently computes the appropriate control voltage by to handle the SMA's non-linear hysteresis and time-varying dynamics. The resulting control signal from Simulink is sent back to the Arduino, where it is converted into a corresponding pulse width modulation (PWM) signal. This PWM signal is then dispatched to the BTS7960 motor driver module. The driver utilizes the PWM input to dynamically switch and regulate the high-current power drawn from the 12 V DC power supply, effectively generating an analog output voltage for the SMA coil. Then, applied voltage across the SMA is precisely controlled, thereby managing its heating and contraction to accurately follow the desired trajectory.

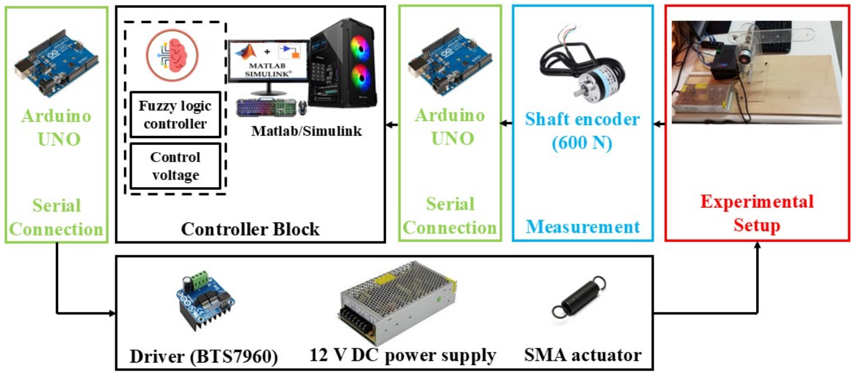

Figure 1. Structure of the used control system.

3. Mathematical model of SMA actuator

Figure 2 shows the schematic of the robotic arm. Based on this schematic, the dynamic equation of motion for the arm is described as follows:

$$I_z\ddot{\theta} + c\dot{\theta} + k\theta + mglcos\theta = \sigma A_{wire} r, \tag{1}$$

The parameters in the above equation are defined as follows: θ is the angular displacement, I_z is the rotational inertia, and l is the distance from the centre of mass. The arm's mass and the gravitational acceleration are given by m and g, respectively. The system's mechanical properties are defined by the torsion spring stiffness k and the torsional damping coefficient c. Finally, the SMA actuator properties are characterized by the stress σ, the cross-sectional area A_{wire}, and the radius of the rotating arm r.

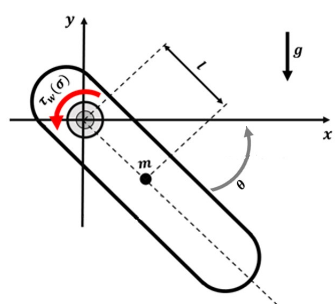

Figure 2. The schematic of the robotic arm.

The constitutive behaviour of the SMA is described by the following model [1]:

$$\dot{\sigma} = E\dot{\varepsilon} + \theta_T\dot{T} + \Omega\dot{\eta}, \tag{2}$$

where E denotes the average Young's modulus, θ_T signifies the thermal expansion coefficient, and Ω represents the transformation coefficient. Also, η describes the phase transformations occurring during heating and cooling. The following equation models the convective heat transfer process in the SMA wire:

$$m_w c_p \frac{dT}{dt} = \frac{V^2}{R} - h_c A_s \left(T - T_\infty\right), \tag{3}$$

in which

$$A_s = \pi \times d \times l_0 . \tag{4}$$

The parameters in this formulation are defined as follows: T is the wire temperature, V is the applied electrical voltage, and T_∞ is the ambient temperature. R denotes the electrical resistance of the wire. The thermal properties are characterized by the mass per unit length m_w, specific heat c_p, and heat transfer coefficient h_c. Finally, the geometric parameters are the wire diameter d, initial length l_0, and surface area A_s.

The hysteresis phenomenon in SMA arises from a reversible phase transformation between two distinct crystalline structures: Martensite (M) and Austenite (A). The evolution of the martensite fraction ζ during the heating (M→A) and cooling (A→M) transformations is described by the following constitutive relations [2],

$$\zeta_{(M\to A)} = \frac{\zeta_M}{2} cos[a'_A\left(T-A_S\right)+b'_A\sigma] + \frac{\zeta_M}{2} \quad , \tag{5}$$

$$\zeta_{(A\to M)} = \frac{1-\zeta_A}{2} cos[a'_M\left(T-M_f\right)+b'_M\sigma] + \frac{1-\zeta_A}{2} \quad , \tag{6}$$

in which

$$a'_A = \frac{\pi}{\left(A_f-A_s\right)}, b'_A = -\frac{a_A}{C_A} \quad , \& \; a'_M = \frac{\pi}{\left(M_S-M_f\right)}, b'_M = -\frac{a_M}{C_M} \quad .$$

. where the martensite fraction ζ is bounded as $0 \leq \zeta \leq 1$. The parameters ζ_M and ζ_A represent the initial martensite fractions for the austenite and martensite phases, respectively, while C_A and C_M are curve-fitting parameters. The phase transformation temperatures are denoted by A_S, A_f, M_S, and M_f, where the subscripts $_S$ and $_f$ indicate the start and finish of transformation, respectively. The state equations for the heating and cooling phases are derived by differentiating Equations (5) and (6) with respect to time [3]:

$$\dot{\zeta}_{(M\to A)} = -\frac{\zeta_m}{2} sin[a'_A\left(T-A_S\right)+b'_A\sigma]\left[a'_A\dot{T}+b'_A\dot{\sigma}\right]. \tag{7}$$

$$\dot{\zeta}_{(A\to M)} = -\frac{1-\zeta_A}{2} sin[a'_M\left(T-M_f\right)+b'_M\sigma]\left[a'_M\dot{T}+b'_M\dot{\sigma}\right]. \tag{8}$$

The strain rate $\dot{\varepsilon}$ of the SMA wire is governed by the following constitutive relation:

$$\dot{\varepsilon} = -\frac{r\dot{\theta}}{l_0}, \tag{9}$$

4. Design of the proposed controller

This section describes the fuzzy control strategy developed for the SMA-actuated robotic arm. the structure of the PD controller to manage the position of the robotic arm is presented as

$$V = \kappa_p e + \kappa_d \frac{de}{dt}. \tag{10}$$

where κ_p and κ_d represent the proportional and derivative gain coefficients of the controller, respectively. Accordingly, the difference between the value measured by the encoder, y, and the reference input, r, is first defined as the tracking error $e = r - y$. Consequently. the error derivative, representing the rate of change of tracking error $\dot{e}$, is subsequently computed. In this respect as depicted in Fig. 3, these two parameters serve as inputs to the fuzzy inference system.

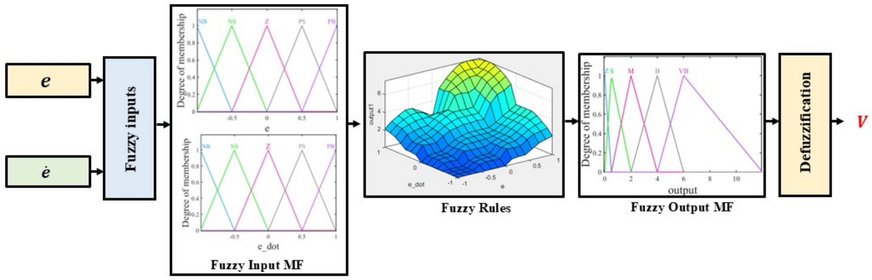

Figure 3. The structure of the FLC.

Utilizing the input membership functions specified in Figure 4, the crisp input values are fuzzified. The system employs five identical variables for both inputs: Positive Big (PB), Positive Small (PS), Zero (Z), Negative Small (NS), and Negative Big (NB). The output membership function of the controller (control voltage), illustrated in Figure 5, utilizes five variables: Very Small (Z), Small (S), Medium (M), Big (B), and Very Big (VB). Due to operational constraints, the voltage range is discretized between 0 and 12 volts. Following this, the fuzzy output is computed by applying the fuzzy inference rules specified in Table 1 to the fuzzified input values. The control rules in Table 1 are derived from classical control principles. For instance:

- If the tracking error is large and negative, and the system is moving away from the reference quickly (with high negative rate of change), then the control input should be significantly reduced to make the system approach the reference value quickly. It is important to note that in this system, which works with voltage and temperature, when the system moves too far from the reference, we need to reduce the temperature or voltage to make the alloy approach its non-aggregated state.
- If the tracking error is small and positive and the system is moving away from the reference slowly (NS), then the control input should be medium to make the system approach the reference value.

Finally, the resulting fuzzy output set was converted into a crisp, actionable value through the centroid of area defuzzification method, which calculates the point under the curve that balances the area of the aggregated membership function.

Table 1. The proposed fuzzy rules.

e	$\dot{e}$				
	NB	**NS**	**Z**	**PS**	**PB**
NL	Z	Z	Z	S	M
NS	Z	Z	S	M	B
Z	Z	S	M	B	VB
PS	S	M	M	B	VB
PB	M	B	B	VB	VB

5. Experimental Results and discussion

In this paper, a robotic arm platform driven by SMA-actuator is designed and constructed for the practical implementation of the proposed controller. The finalized setup is shown in Fig. 6. In this structure, the angular displacement of the platform is measured by two phase encoder, sampled at 50 Hz. Two Arduino UNO R3 boards function as the input-output (I/O) interface, acquiring sensor data and issuing the control signal. In this architecture, the control input calculations are executed on a workstation featuring an Intel® Core. i9-12900K processor (3.2 GHz base frequency, 30 MB cache). Sensor output is sent via a serial port to Simulink software, where the control voltage is calculated. The computed control voltage is converted to PWM format and transmitted to a BTS7960 driver operating at 12V DC. This driver subsequently applies the corresponding control voltage to the SMA actuator, thereby closing the hardware in the loop (HIL) implementation.

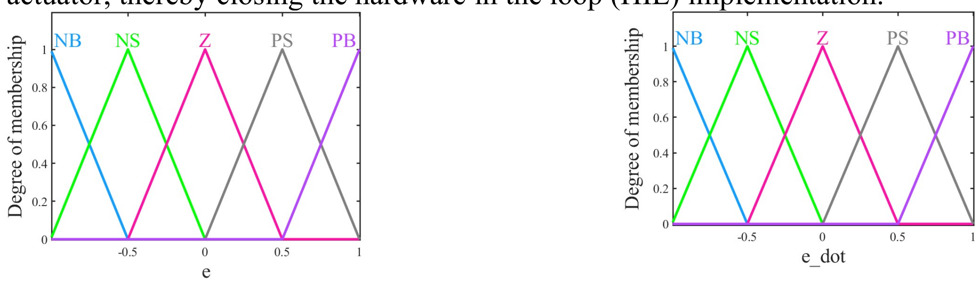

(a) (b)

Figure 4. Input membership function, (a) Tracking error, (b) Tracking error derivative.

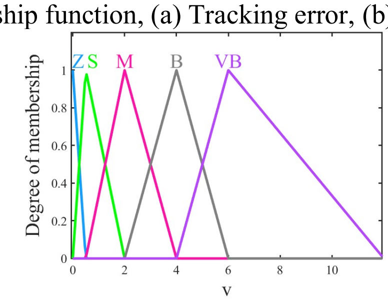

Figure 5. Output membership function.

(a) (b)

Figure 6. Test equipment, (a) Workstation, (b) Test platform.

In this section, to verify the effectiveness of the proposed fuzzy control strategy in real conditions, experimental studies are conducted on the SMA-based robotic manipulator platform. Initially, appropriate values of the proportional and derivative gains, κ_p and κ_d are selected through manual tuning. In Figure 7, three different values of κ_p are tested. As shown in Fig. 7(d), by comparing the root-mean-square (RMS) tracking error and the corresponding control input, the best performance is obtained when $\kappa_p = 100$. Subsequently, for the constant value of $\kappa_p = 100$ the derivative gain κ_d is adjusted to improve the transient response and reduce oscillations in the output. As shown in Figure 8, three values of κ_d are examined, and the optimal performance is achieved for $\kappa_d = 1$. This value minimizes the RMS of both the tracking error and the control effort.

Figures 9 present the experimental results of the fuzzy PD controller compared with those of the conventional PD controller for Test-2. As shown in Figures 9**,** the proposed fuzzy approach provides superior tracking performance for the periodic reference trajectory. The RMS values of the tracking error and control signal is summarized in Figures 9(d), confirming that the fuzzy PD controller achieves smaller tracking error and smoother control effort than the traditional PD controller in both tests.

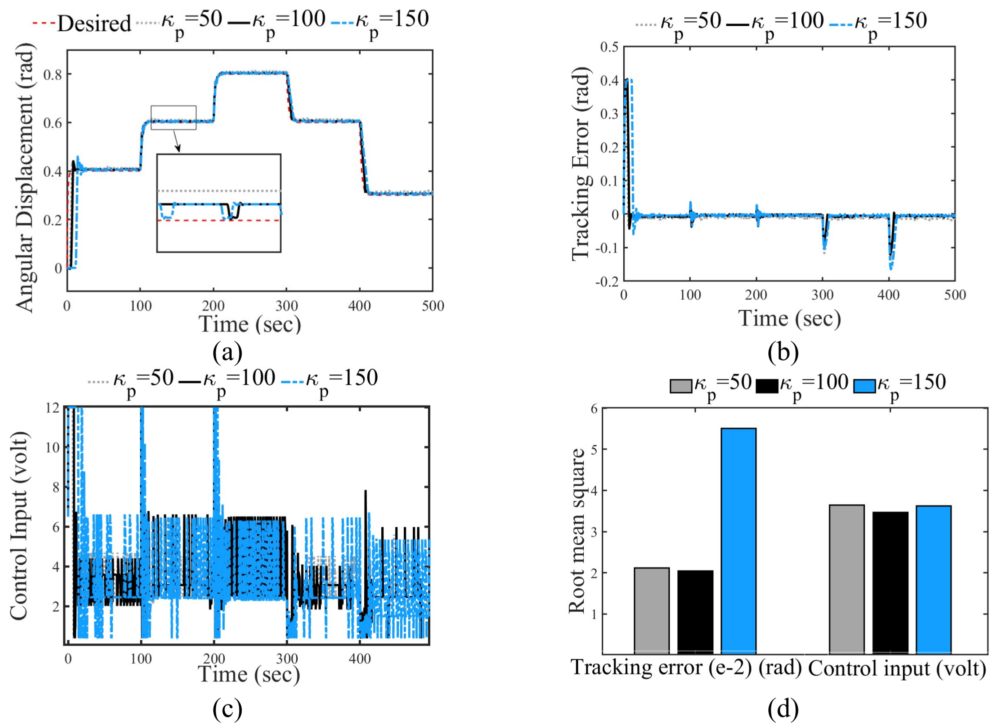

Figure 7. Comparative results for different κ_p in test-1, (a) Angular displacement, (b) Tracking error, (c) Control input, (d) RMS of outputs.

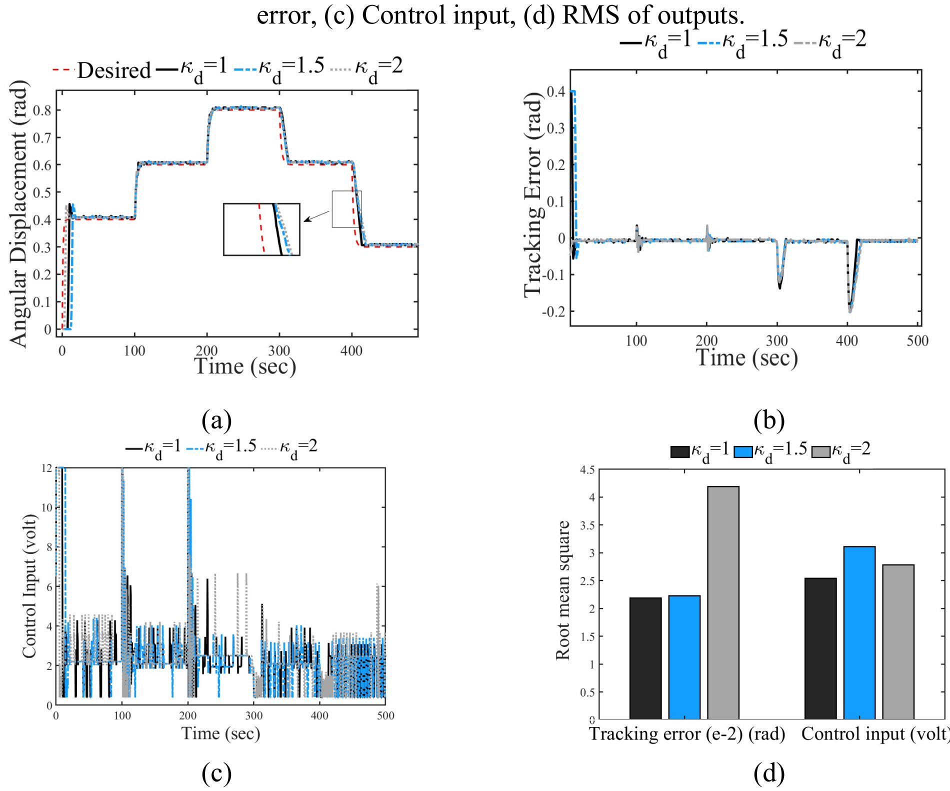

Figure 8. Comparative results for different κ_d in test-1, (a) Angular displacement, (b) Tracking error, (c) Control input, (d) RMS of outputs.

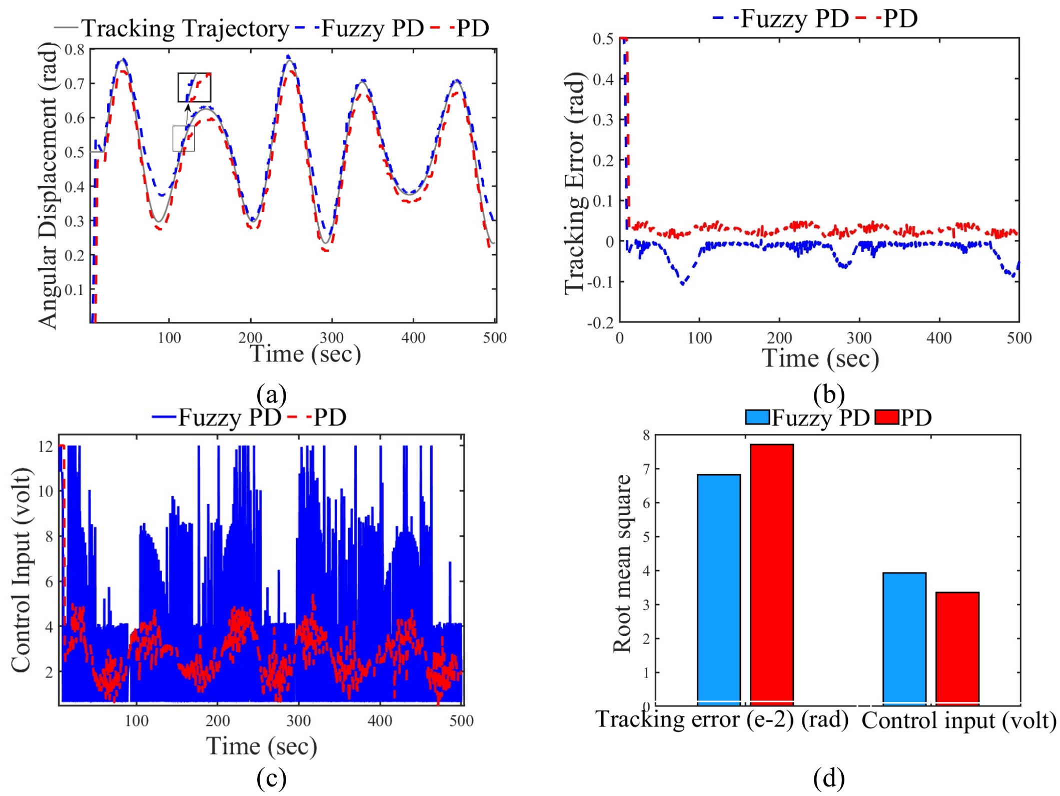

Figure 9. Comparative results of the fuzzy PD and conventional PD controllers, (a) Angular displacement for Test-2, (b) Control input for Test-2, (c) Angular displacement for Test-2, (d) Control input for Test-2.

6. Conclusion

This paper presented the design, and experimental validation of a fuzzy logic controller for position control of a robotic arm actuated by a SMA. The experimental results demonstrated that the proposed controller achieves accurate trajectory tracking and improved performance compared with a conventional PD controller. Overall, the findings confirm that the fuzzy logic PD controller offers a reliable control solution for SMA-driven robotic manipulators under both step and periodic trajectories

1. M. M. Shahir, M. Mirzaei, M. Farbodi, & S. Rafatnia, "Estimation of shape memory alloy actuator dynamics to design reduced-order position controller with input saturation", *IET Control Theory & Applications*, *18*(10), 1301-1313 (2024).
2. M. M. Shahir, M. Mirzaei, M. Farbodi, & S. Rafatnia, "Extended state observer-based feedback linearization control of shape memory alloy actuator: design and experiment", *International Journal of Dynamics and Control*, *12*(7), 2447-2458 (2024).
3. M. M. Shahir, M. Mirzaei, S. Rafatnia, Z. A. Sisi, & S. Jamshidi, "Super twisting sliding mode control of a robotic manipulator actuated by shape memory alloy: Design and experiment", *2023 11th RSI International Conference on Robotics and Mechatronics (ICRoM)*, (pp. 419-424). IEEE (2023, December).
4. S. F. Hoseini, S. A. MirMohammadSadeghi, A. Fathi, & H. M. Daniali, "Adaptive predictive control of a novel shape memory alloy rod actuator", *Proceedings of the Institution of Mechanical Engineers, Part I: Journal of Systems and Control Engineering*, *235*(3), 291-301 (2021).
5. M. Jin, J. Lee, & K. K. Ahn, "Continuous nonsingular terminal sliding-mode control of shape memory alloy actuators using time delay estimation", *IEEE/ASME Transactions on Mechatronics*, *20*(2), 899-909 (2014).
6. Z. J. Patterson, A. P. Sabelhaus, & C. Majidi, "Robust control of a multi-axis shape memory alloy-driven soft manipulator", *IEEE robotics and automation letters*, *7*(2), 2210-2217 (2022).
7. M. Liu, Z. Zhao, & L. Hao, "Prescribed performance model-free adaptive sliding mode control of a shape memory alloy actuated system", *ISA transactions*, *123*, 339-345 (2022).